http://dx.doi.org/10.1109/ICNN.1995.488875

Zaknich, A. and Attikiouzel, Y. (1995) Detection of sodium oxalate needles in optical images using neural network classifiers. In: IEEE International Conference on Neural Networks, 27 November - 1 December, Perth, Western Australia, pp. 1699 - 1702.

Detection of Sodium Oxalate Needles in Optical Images Using Neural Network Classifiers

Anthony Zaknich, Member IEEE, Associate Member of AES
Yianni Attikiouzel, Senior Member IEEE, Fellow IEE, Fellow IEAust

Centre for Intelligent Information Processing Systems (CIIPS),
Department of Electrical and Electronic Engineering,
The University of Western Australia, Nedlands 6907, Western Australia

Abstract

A description is given of a PC based system for the automatic detection, counting and sizing of sodium oxalate needles in optical microscope images predominated by a background of hydrate particles. The system is primarily based on a neural network classifier which is fed by a feature vector derived from greyscale dynamically thresholded binary images. A Backpropagation neural network (BPN) was adopted for technical reasons but any of the other neural network classifiers could have been used. Comparative results are given for the Backpropagation, Probabilistic (PNN), General Regression (GRNN) neural networks and a Gaussian model which show the utility and validity of the neural network approach.

Alcoa of Australia Limited uses the Bayer process to refine alumina. This involves the digestion of gibbsite from bauxite in a caustic soda solution and subsequent reprecipitation of the gibbsite in a continuous precipitation circuit. The gibbsite is calcined at 1000 $^{\circ}$C and shipped to smelters. Some of the organics that are introduced into the Bayer liquor via the bauxite form sodium oxalate. The liquor in the precipitation circuit is saturated with respect to sodium oxalate. In this saturated state there is a likelihood that oxalate will nucleate as needle-like crystals and co-precipitate with the gibbsite (hydrate) particles which is not desirable. Monitoring of critical areas in precipitation is undertaken daily by production personnel to give an early warning for the presence of oxalate. They prepare slides and inspect them using optical microscopy for the presence and number of needles in random fields of view. This technique is very operator dependent as some skill is required to recognise the needles.

To reduce operator subjectivity a PC based automated system for discriminating the oxalate crystals from the hydrate particles, and subsequently counting and sizing the oxalate needles, was developed by CIIPS [1]. The system was based on a neural network classifier trained to identify needles in greyscale dynamically thresholded binary images. The optimal threshold is automatically computed for each image. Under normal operation the system takes the resulting binary images and firstly clears objects which are too small or too large. Then, the remaining objects are classified as either being needles or not. If they are classified as needles their lengths and widths are measured and recorded. The system's main task is to reliably and accurately discriminate needles in a background of many hydrate particles. It is able to function automatically with both normal and polarised light sources and with both white on black and black on white views. Polarised light allows the operator to manually filter out many of the hydrate particles in the background before the images are captured.

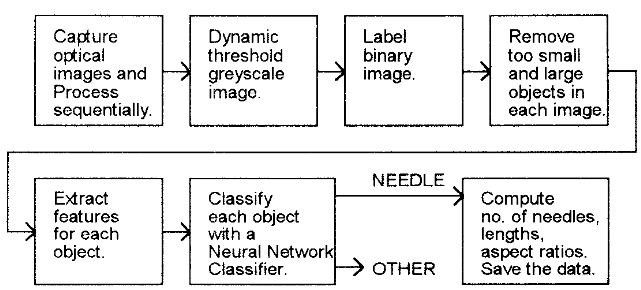

FIGURE 1: Oxalate Needle Counting System Block Diagram

The system hardware includes a standard IBM compatible 80386/33 PC or higher, a PROVIDEO 100 frame grabber card set to 512 by 352 pixels resolution, a Panasonic WV-CL700 video camera with a TV relay lens

1x/16 and a Nikon OPTIPHOT microscope with a x20 objective lens. The system software was written in Borland C version 3.0 for the DOS environment with at least 600 MBytes of free RAM. A typical image illuminated with normal light takes approximately 4 minutes to process on an 80486/33 PC whereas an image illuminated with polarised light takes approximately 45 seconds. Figure 1 shows the system block diagram showing the main processing stages.

An example of the system's operation on a normally lighted image with three oxalate needles present is shown in the sequence of three images shown in Figures 2 to 4. The first image is the original greyscale image, the second is the binary image just before the feature extraction stage and the final one is the resulting binary image after all the non-needles have been eliminated.

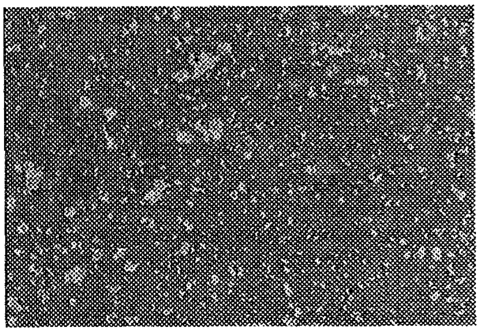

FIGURE 2: Needles in a background of hydrate particles

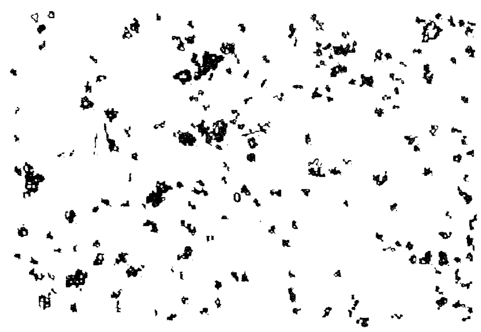

FIGURE 3: The preprocessed binary image

FIGURE 4: The 3 oxalate needles identified

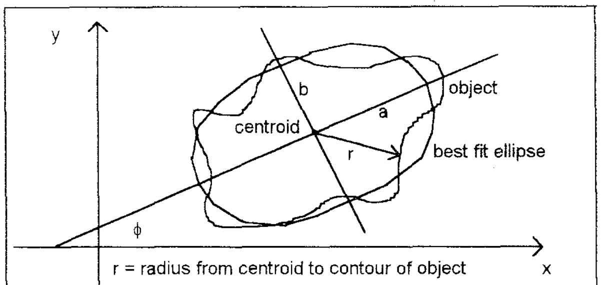

FIGURE 5: Ellipse Fitting Diagram

After the initial preprocessing stage each of the objects in the final binary image are identified and features are extracted from them to use for the needle classification. If the object is classified as a needle it is retained in the binary image else it is eliminated. Before this is done each object is dilated and then eroded to ensure that any holes in it are filled in to provide a solid silhouette. The features adopted for the system were chosen to minimise intra-class variance and maximise inter-class variance. The final feature vector consisted of 14 features extracted from each two-dimensional binary silhouette as follows:

1) Shape factor.
2) (minimum) / (maximum radius from centroid to the boundary).
3) (mean) / (maximum radius from centroid to the boundary).
4) (standard deviation) / (maximum radius from centroid to the boundary).
5) First normalised spectral frequency bin of 8 radii sampled at $2\pi/8$ radian intervals.
6) Second normalised spectral frequency bin of 8 radii sampled at $2\pi/8$ radian intervals.
7) Third normalised spectral frequency bin of 8 radii sampled at $2\pi/8$ radian intervals.
8) Fourth normalised spectral frequency bin of 8 radii sampled at $2\pi/8$ radian intervals.
9) (number of pixels in contour) / (total area).
10) (maximum radius from centroid to the boundary) / (total area).
11) (minor ellipse axis length) / (major ellipse axis length), for best fitting ellipse.
12) (object area inside ellipse) / (total area).
13) (number of pixels in skeleton -1) / (total area).
14) Mean standard deviation around line of best fit to the skeleton.

The shape factor is defined as (4π area) / (contour length)^2. The ellipse parameters were computed from the two-dimensional moments [2] of the binary image of the object as follows:

The equation of an ellipse is: $(x/a)^2 + (y/b)^2 = 1$, where:
a = major ellipse radius from the centroid, b = minor ellipse radius from the centroid and
x and y are the two-dimensional coordinate variables with the centroid at the origin.

The two-dimensional moments of a binary object are defined as:

$m_{pq} = \Sigma\Sigma\, x^p y^q$, where:

$a = [\,(m_{20} + m_{02} + ((m_{20} - m_{02})^2 + 4\,m_{11}^2)^{0.5}) / (0.5\, m_{00})\,]^{0.5}$

$b = [\,(m_{20} + m_{02} - ((m_{20} - m_{02})^2 + 4\,m_{11}^2)^{0.5}) / (0.5\, m_{00})\,]^{0.5}$

$\phi = 0.5 \tan^{-1}(2\, m_{11} / (m_{20} - m_{02}))$, where: ϕ = angle of the major ellipse axis.

The x and y here are the image coordinates.

The neural network classifier output dimension was two where class zero (non-needle) was represented by the vector (0.9, 0.1) and class one (needle) by the vector (0.1, 0.9). The objects are classified as needles only if feature numbers 2 and 6 are both less than 0.33 and if the feature vector is classified as such by the pretrained neural network classifier. The neural network used in the system was a three layer Backpropagation Network (BPN) having fourteen input nodes, seven hidden nodes and two output nodes (14-7-2). Any neural network classifier would have been suitable but the BPN was finally chosen because it has a fairly efficient implementation for software applications. The BPN classifier was trained and tested using two independent vector sets, a training and testing set, composed of random non-needle and needle vectors gathered from images illuminated by both non-polarised and polarised light. Both the training and testing sets had 405 non-needles and 56 needles.

The BPN classifier after 400,000 training iterations taking 43 minutes and 19.2 seconds achieved the following results. Single vector execution time on an 80386/33 PC was 0.003449 seconds per vector.

True \ System	0	1
0	405	0
1	5	51

Maximum Training Accuracy = 98.92%

True \ System	0	1
0	403	2
1	10	46

Maximum Testing Accuracy = 97.40%

Classification Confusion Matrices for the BPN

The standard PNN [3] produced the results shown below. It took 56.41 seconds to do one training pass and the vector execution time was 0.1221 seconds per vector. If a General Regression Neural Network (GRNN) [4,5] is used as a classifier the number of training data points is taken to be in proportion with the a priori probability of occurrence and the accuracy improves slightly as shown below. The GRNN used as a classifier is very similar to the PNN. The true a priori probability of occurrence of the needles is in fact much less than indicated by the numbers in the training and testing sets as they occur only occasionally under normal plant operation.

True \ System	0	1
0	395	10
1	5	51

Maximum Testing Accuracy = 96.75%
σ = 0.084 -> 0.088

Classification Confusion Matrix for the PNN

True \ System	0	1
0	403	2
1	10	46

Overall Testing Accuracy = 97.40%
σ = 0.1030

Classification Confusion Matrix for the GRNN

A single multi-dimensional Gaussian model [6] for each class which assumes that the numbers of the training data points are in proportion to their class a priori probability of occurrence produces the following classification results. This model was trained in 0.88 seconds and the vector execution time was 0.003818 seconds per vector.

True \ System	0	1
0	364	41
1	0	56

Maximum Training Accuracy = 91.11%

True \ System	0	1
0	361	44
1	1	55

Maximum Testing Accuracy = 90.46%

Classification Confusion Matrices for Gaussian Model

The BPN produced the most accurate and efficient software classifier realisation, although, the GRNN produced equal testing results to the BPN. The BPN however, required the longest training time. The PNN showed a slightly lower accuracy because it takes no account of the a priori probability of occurrence of each class vector as the other networks do. Even though in this application the BPN was chosen for implementation, the maximum accuracy of the GRNN was used as a guide to train the BPN to the expected maximum performance. In this application the reduction of the false positives (ie. false needle detection) was more significant than maximum true positive accuracy. Both the BPN and GRNN achieved the minimum false positives and maximum true positives for the testing set. To ensure the reduction of false positives in the final system all objects having features number 2 and 6 greater than 0.33 were rejected before passing to the BPN classifier.

Conclusions

The classification results achieved should not be interpreted as a specification of the system's actual performance because relatively few training and testing vectors have been collected from a complex process which is able to produce a large variety of oxalate and hydrate shapes and sizes. Many more training vectors from typical images need to be collected before the system can be said to be adequately trained. What the results do show however, is that after more comprehensive training the neural network classifier system is expected to work well. The 14 features based on binary image information alone appear to be quite adequate to achieve good discrimination. There seems to be no need to consider more complex features from the original greyscale image information which would involve more complexity and computation time. Due to insufficient training data no attempt to reduce the features to an optimal set has been made at this stage. No special allowance was made for touching objects but the classifier was able to correctly classify needles with small touching hydrate particles as can be seen in two out of three of the needles in the example image.

Acknowledgments

Alcoa of Australia Limited provided the process data, expert knowledge and access to plant facilities which were essential for the successful completion of this work. A very special thanks to Alcoa personnel Gerald Roach and John Cornell who between the years 1992 to 1994 have directly assisted CIIPS on this and other research projects related to Alumina industry.

[1] Zaknich, Anthony and Cornell, John, "Application of neural networks to image analysis in the alumina industry", Image Analysis Seminar 94, Western Australian Society for Electron Microscopy, Espanade Hotel, Fremantle, Western Australia, 1st September 1994, pp. 27-37.

[2] Teague, M. R., "Image analysis via the general theory of moments", Journal of the Optical Society of America, Vol. 70 No 8., August 1980, pp. 920-930.

[3] Specht, D. F., "Probabilistic neural networks", Neural Networks, Vol 3, 1990, pp. 109-118.

[4] Specht, D. F., "A general regression neural network", IEEE Transactions on Neural Networks, Vol. 2, No. 6, November 1991, pp. 568-576.

[5] Zaknich, Anthony, deSilva, Christopher and Attikiouzel, Yianni, "The probabilistic neural network for nonlinear time series analysis", IEEE International Joint Conference on Neural Networks (IJCNN), Singapore, 17-21st November 1991, pp. 1530-1535.

[6] Zhang, Y., deSilva, C. J. S., Togneri, R., Alder, M. and Attikiouzel, Y. A., "A HMM/EM speaker-independent isolated word recogniser", Journal of Electrical and Electronics Engineering, Australia, Vol. 12, No. 4, December 1992, pp. 334-339.